

Proximity and Antenna Orientation Effects for Large-Form-Factor Devices in a Reverberation Chamber

Willem T. C. Burger^{1,2}, Kate A. Remley², Christopher L. Holloway², John M. Ladbury²

¹*Electromagnetics Group, Technical University Eindhoven, 5612AZ Eindhoven, The Netherlands*

²*National Institute of Standards and Technology, Boulder, CO USA*

email: kate.remley@nist.gov, phone:303-497-3652

Abstract—Recent research has shown that large-form-factor devices can affect radiated power measurements in a reverberation chamber due to absorption by lossy material present in the device. In this paper, these effects are explained and related to the angular orientation and proximity of the antenna associated with the large-form-factor load in the reverberation chamber. It is shown that RF absorption rather than physical shadowing of an antenna by the object under test is the origin of the proximity effect.

I. INTRODUCTION

With the increased proliferation of large-form-factor, machine-to-machine (M2M) communication technology, the interest in use of reverberation chambers (RCs) for testing and characterization of these devices has grown. In particular, the low-cost scalability of RCs, in comparison to anechoic chambers, has made RCs interesting as a test environment for large-form-factor devices. In [1]-[5], some applications of the RC as a test environment can be found.

In an ideal RC, the fields in the chamber, when averaged, are spatially uniform and isotropic, provided they are well stirred and in a highly overmoded condition [5]. This property of spatial uniformity is highly dependent on the loading of the chamber. Certain devices-under-test (DUTs) can load the chamber, absorbing a portion of the energy present in the chamber and decreasing its spatial uniformity [6]-[8]. Thus, the loading of a reverberation chamber may have an impact on the received-power measurement of a DUT, as well as affecting the measurement uncertainty of the received-power measurement. In [9] it was shown that large-form-factor devices that load the chamber decrease the measured received power and increase the measurement uncertainty when antennas are placed in close proximity to the load to a greater degree than elsewhere in the chamber. This “proximity effect” was shown in [9] to be caused by a physically large load “blocking” (absorbing) the incoming radiation to an antenna close to the load from a certain direction or, conversely, blocking radiation emanating from the antenna in that direction.

In [10], a method is described to measure the total radiated power (TRP) of a DUT with a reverberation chamber. In general, to ensure a TRP measurement has a low uncertainty, the field distribution in the chamber must be as uniform as

possible. This ensures that a measurement is independent of the exact location of the DUT and the receive antenna within the working volume of the RC. The standard further illustrates that the spatial uniformity of a chamber can be represented by the standard deviation of the mean field for measurements made at various locations throughout the chamber. A low standard deviation of the mean field indicates that there is a sufficient number of modes in the chamber, the paddle is large enough to interact with these modes, and the set of independent data points is sufficiently high. Thus, for a heavily loaded chamber (with a correspondingly high standard deviation of the mean field) more data points (i.e., more averaging over paddle positions or positions in the RC) are required in order to achieve the same accuracy as for an unloaded chamber. This method for characterizing spatial uniformity, while certainly useful for measurements in loaded chambers in general, is not sufficient to describe the effects that close proximity of the DUT or reference antenna to a load in a chamber has on uncertainty, as is shown in [9].

It is this proximity effect, the blocking of radiation by large-form-factor absorbing objects that will be the main focus of this paper. The influence on received-power measurements will be shown for various degrees of proximity of an antenna to a chamber load as well as for various antenna orientations with respect to the load. The antenna and load together represent a large DUT partially made out of lossy material (one could imagine, for example, a vending machine incorporating large amounts of polymer-based insulating material). From these measurement results, we discuss best practices for design of large M2M communicating devices with respect to the placement of antennas on such devices. The measured results are compared with theoretical system models, leading to a generalization of the placement guidelines to incorporate various antenna types, such as monopoles, dual-ridge horns or patch antennas.

II. CALCULATING TOTAL RECEIVED POWER

In order to calculate the total received power (or a “power-like quantity”), the scattering parameter S_{21} is used. This scattering coefficient is the transfer function of the radio-propagation environment [1] and is shown in [11] to be propor-

tional to the rectangular field components in the reverberation chamber. In addition to calculating the power from the measured S_{21} , it is also necessary to correct for antenna mismatch, shown in [12]–[14]. Note that the “power”, as defined in this paper, is a relative value, as the S-parameters measured by the vector network analyzer (VNA) are dimensionless. To calculate the actual power, further calibration with a power meter is required. This is outside the scope of this paper.

Reverberation chambers are not ideal, resulting in two components for S_{21} : the stirred and unstirred components. The stirred component is that part of the total field that interacts with the rotating paddle, and the unstirred component is the part of the field that does not. For example, the direct line-of-sight component from a transmitter to a receiver is unstirred. The unstirred component is considered to be deterministic and is superimposed on the stochastic electromagnetic field [11]. The received power incorporating both stirred and unstirred components is given by [1]:

$$\langle |S_{21}|^2 \rangle = \frac{\langle |S_{21}|^2 \rangle}{(1 - \langle |S_{11}|^2 \rangle)(1 - \langle |S_{22}|^2 \rangle)}, \quad (1)$$

where S_{21} has been corrected for antenna mismatch. The terms $\langle |S_{11}|^2 \rangle$ and $\langle |S_{22}|^2 \rangle$ are the free-space reflection coefficients of the transmit antenna and the receive antenna [15], [16]. The averages taken in this equation are ensemble averages over all stirrer positions.

In [1], it was described how the stirred component of the field in an RC can be calculated from the scattering parameters. The unstirred components are related to the mean value of S_{21} , and can be simply subtracted from S_{21} . As such, the stirred power can be described by [1] as

$$\langle |S_{21}|^2 \rangle_{stirred} = \frac{\langle |S_{21} - \langle S_{21} \rangle|^2 \rangle}{(1 - \langle |S_{11}|^2 \rangle)(1 - \langle |S_{22}|^2 \rangle)}. \quad (2)$$

In general, the received power given in (1) and (2) is that measured at the antenna ports. To obtain the received power at the input ports of the antenna, (1) and (2) must be corrected for the efficiencies of the two antennas, see [12]. This is not considered in this paper, as the only metric of interest is the relative change of S_{21} that results from different loading conditions.

III. EXPERIMENTAL SETUP AND RESULTS

A. Received power — monopole antenna

In order to examine the influence of antenna orientation and proximity with respect to large-form-factor loads in the chamber, received-power measurements were conducted in a rectangular reverberation chamber having dimensions of 4.6 m x 3.1 m x 2.8 m. For the measurement, a dual-ridge horn antenna, designated as the transmit antenna, was placed in the chamber at close proximity to the stirrer, pointed directly at the paddles, as in [1]. The second antenna, designated as the receive antenna, was an in-house-manufactured monopole antenna, with a ground plane of 0.2 m x 0.2 m and a half-wavelength radiating element tuned to 1.9 GHz. For each measurement, the monopole was placed at a set distance, from

15 cm to 65 cm in increments of 5 cm, and a set angle, from 0° to 180° in increments of 22.5° , with respect to a stack of blocks of absorbing material placed in the chamber. (See Fig. 1 for an overview of the chamber setup and Fig. 2 for a illustration of the measurement setup parameters.) For the measurement, 0° was defined as the position in which the radiating element of the monopole was pointing directly at the chamber load, and 180° as the position in which the monopole was pointing directly away from the load. The absorber blocks were carbon-loaded material with dimensions of 0.6 m x 0.6 m x 0.15 m. For each measurement either zero, four, eight, 12 or 14 blocks were placed in the chamber. With a VNA, the four scattering parameters S_{11} , S_{12} , S_{21} and S_{22} were measured over a frequency range of 1.5 GHz to 2.5 GHz, over 16000 points at an output of -8 dBm. The stirrer was rotated in 72 increments of 5° each step, to complete a full 360° turn.

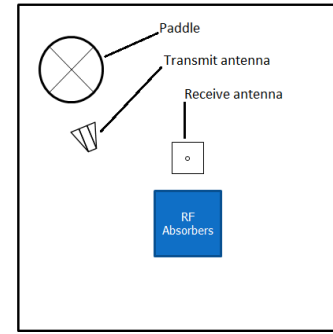


Figure 1. Reverberation Chamber setup

For each configuration of chamber load, antenna orientation, and antenna position, the S-parameters were measured. The received power was then compared to the received power of the measurement taken 65 cm from the absorber and with the antenna pointed 180° away from the absorber. The latter represented a “baseline” measurement for which the influence of the absorber in terms of blocking radiation from the monopole was minimal. These comparisons between the “baseline” and the various measurements form the basis of the guidelines for antenna placement discussed later in this paper.

Using data on measurement uncertainty stemming from chamber loading and measurement reproducibility from earlier measurements [9] and the techniques described in [12], the uncertainties presented in Table I were calculated. In this table, the uncertainty $U_{L,total}$ was calculated based on both measurement system reproducibility, represented by $U_{L,measurement}$, and the uncertainty arising from the decrease in spatial uniformity due to the presence of loading in the chamber, represented by $U_{L,loading}$. Note that $U_{L,loading}$ was found from measurements made at multiple antenna locations and illustrates the need for position stirring in loaded RCs. The uncertainty stemming from VNA drift was not taken into account, as this was determined in [9] to be negligible. The metric for determining whether the blockage of radiation was significant was chosen to be the measurement uncertainty of S_{21} . Thus, if the difference in received power with respect to

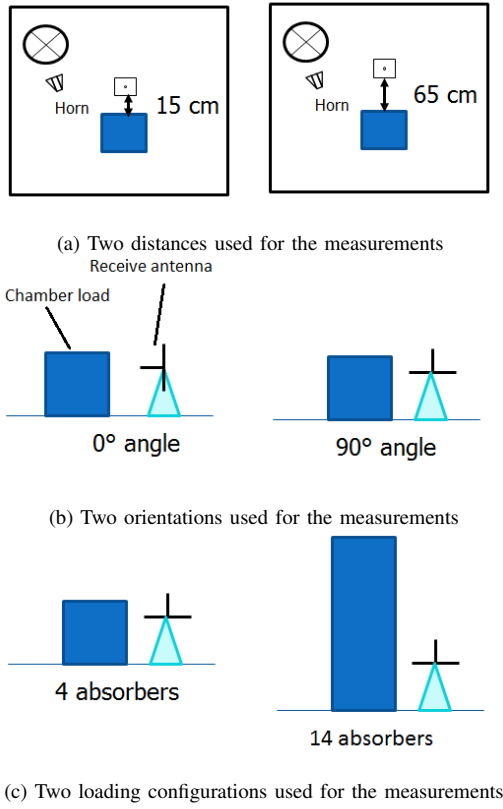


Figure 2. Measurement setup parameters

the baseline was larger than the measurement uncertainty, the effect was deemed significant.

In Figs. 3 and 4, the graphs show the influence of proximity and antenna orientation on measured received power. In Fig. 3, the received power is shown for various loading configurations with the receive antenna 15 cm from the absorbers and with the antenna oriented to 0°, pointing at the absorber. In Fig. 4 the receive antenna is placed at a 65 cm distance and oriented to 180°. In these figures it can be seen that for identical loading conditions, the received power in the 0°, 15 cm case is lower overall than for the 180°, 65 cm case, confirming and expanding upon results from [9]. For the zero absorber case, the received power is the same (within $U_{L,total}$) in the two figures, confirming the spatial uniformity of the unloaded chamber. Note that for a full TRP measurement, a calibration step corrects for the difference in the received power due to loading. Proximity effects will not be corrected, however.

In Fig. 5, the proximity effect due to the absorbers is further illustrated for two loadings. In these figures, the difference between the received power measured for a certain receive antenna proximity and angle configuration and that at the “baseline,” as defined in the previous section, is shown. In addition, a plane representing the value of the measurement uncertainty at that loading configuration is plotted. As can be seen, the attenuation of the signal due to blockage by the absorbers decreases sharply as distance and angle increase. Furthermore, the measurement uncertainty threshold in each

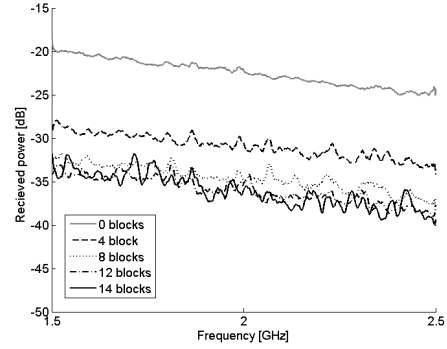


Figure 3. Total received power for various loading configurations at distance 15 cm, angle 0°.

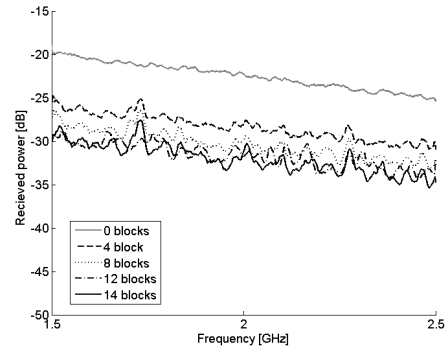


Figure 4. Total received power for various loading configurations at distance 65 cm, angle 180°.

figure indicates for which angles and which distances the proximity effect ceases to be significant. It can be seen from Fig. 5(a), for example, that if one places the receive antenna 50 cm from the stack of four absorbers, an antenna orientation of 90° will be sufficient to render the effect of blocking negligible. However, Fig. 5(b) shows that in the case of 14 absorber pieces, an antenna orientation of at least 140° degrees is required regardless of the proximity to the absorber. In each case, however, the additional attenuation due to the proximity effect is greater than the threshold of significance for a majority of the tested positions and orientations. In the cases of eight blocks or more, the additional attenuation can reach over 4 dB, indicating a significant loss of signal power at the load.

B. Received power - horn antenna

To test the hypothesis that antennas with a higher gain are more affected by the proximity effect, a second set of measurements was conducted, using a standard gain horn tuned to 1.9 GHz, instead of the monopole, as the receive antenna. For this experiment, all tests were conducted with the radiating element of the horn set 50 cm from the absorber and only three antenna orientations were used: 0°, 90° and 180°.

Fig. 6 shows the effect of radiation blockage by absorbers on the received-power measurement of the standard gain horn

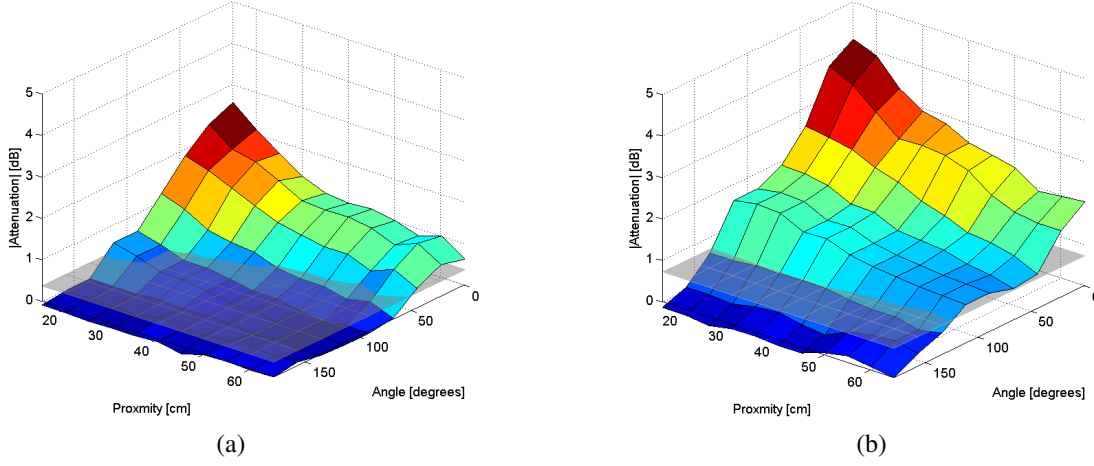


Figure 5. Reduction in received power compared to the baseline for: (a) four absorber blocks, and (b) 14 absorber blocks.

antenna along with results for the monopole antenna for the same distance, angle and loading configurations. As can be seen, at 50 cm and for small angles with respect to the absorber, the decrease of received power from the baseline is larger than that for the monopole antenna. Furthermore, it can be seen that the additional attenuation due to blockage for the horn drops to zero after 90° . This shows that a high-gain antenna can be affected more by the proximity effect than a lower-gain antenna, due to its narrower beam width. Similarly, the horn antenna also shows a sharper drop in attenuation as a result of changing antenna orientation than that for the lower gain antenna. Note also that the results for eight, 12 and 14 absorbers nearly overlap perfectly. This is due to the narrow beam of the standard gain horn.

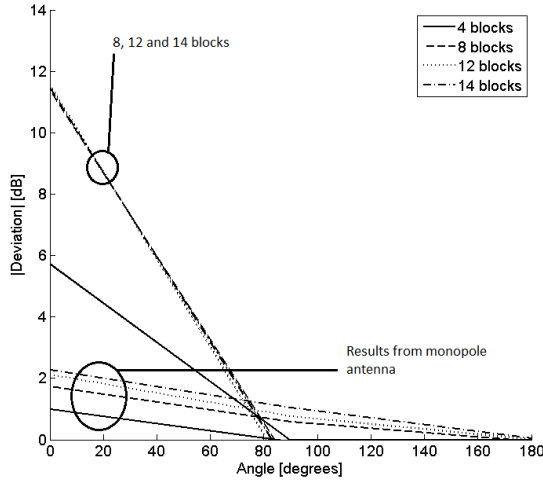


Figure 6. Effects of blockage by absorber for standard gain horn and monopole antenna, at 50 cm distance.

C. Antenna placement within chamber

In addition to the measurements to determine the extent of the proximity effect, measurements were conducted to determine whether the placement of the antenna at different positions around the absorber would yield different results. For

this measurement, the monopole was sequentially placed at a fixed position, 15 cm and at a fixed angle of 90° , at each face of the block for four absorbers (named North, West, South and East). Fig. 7 illustrates the measurement setup. Similar to the measurements described above, the scattering parameters were measured for the same frequency range, power output and number of stirrer positions. The received power at each position was computed, and the results compared.

Fig. 7 shows the received-power measurement taken for the four different positions around the absorber. Table II shows the mean power, averaged over paddle position and frequency, for each of these measurements. As can be seen, there is no significant difference between the measurements at different points around the absorber, for a given distance and antenna orientation. From this result it can be concluded that the relative position and orientation of the antenna with respect to the load influence the proximity effect, not the general position of the antenna in the chamber. Thus, the absorbing load removes power from the fields within the chamber no matter what position the receive antenna occupies within it. A similar result would be expected for anechoic chambers as well.

IV. COMPARISON WITH THEORETICAL MODELS

Using a finite element simulator, a model for the monopole used in the measurements was designed. In Fig. 8, the resulting antenna pattern is shown. Next, geometry was used to determine the section of the antenna pattern likely to be blocked by a load of a given size for each antenna orientation and proximity to the load. This is indicated by the black shaded section of Fig. 8. This section was integrated over azimuth (ϕ) and elevation (ϑ) and divided by the integration over the entire antenna pattern. Thus, the relative amount of power blocked by the absorber and not interacting with the chamber can be approximated by:

$$\frac{\int_{\phi_1}^{\phi_2} \int_{\vartheta_1}^{\vartheta_2} (1 - |R|^2) P \sin \theta d\vartheta d\phi}{\int_0^{2\pi} \int_0^\pi P \sin \theta d\vartheta d\phi}, \quad (3)$$

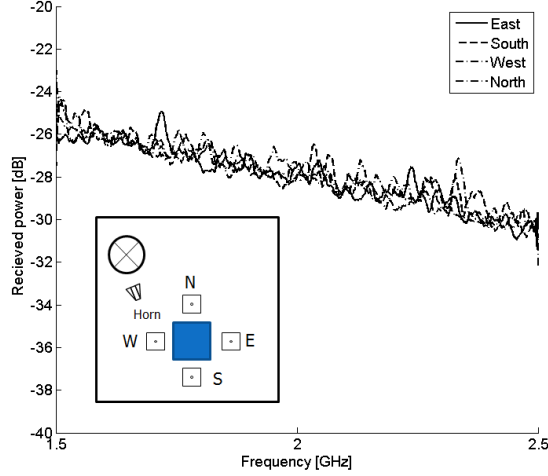


Figure 7. Total received power for various antenna placements, four absorber blocks.

where P represents the monopole antenna pattern, $[\vartheta_1, \vartheta_2]$ and $[\phi_1, \phi_2]$ the boundaries of the section of the antenna pattern blocked by the absorbers, and R the reflectivity of the absorber block as a function of incident angle acting as a weighting vector for the antenna pattern at each angle point. R can be represented by [17]: $|R(\vartheta, \phi)|^2 = \frac{|R_{TE}|^2 + |R_{TM}|^2}{2}$, with $|R_{TE}|^2$ and $|R_{TM}|^2$ representing the transverse electric (TE) and magnetic (TM) planewave reflection coefficients. For the calculation of $|R(\vartheta, \phi)|^2$ it was assumed that the absorber was infinitely thick and that the permittivity was $\epsilon_r = 2.0 - j0.14$, which is typical for this type of absorber [18].

In Fig. 9 an example of the estimated proportion blocked by 14 absorber blocks plotted against angle and proximity can be seen. In Fig. 10, the difference in decibels between the actual measurements and the theoretical model is shown for two loadings. The figures show that the model and the measurements differ by up to 1 dB, which is more than the measurement uncertainty for each loading case, but still low enough to provide confidence in the use of the model as a predictive tool in certain applications. As such, it helps physically explain how the absorbers block radiation from reaching the antenna, essentially preventing energy from one antenna in the RC from coupling into the other one. In any case, the model as it stands follows the trends of the measurements. As such, it helps physically explain how the absorbers block radiation from reaching the antenna, preventing antenna-to-antenna coupling.

V. CONCLUSIONS AND FURTHER STUDY

The results presented in Section III suggest that the proximity effect can have a significant influence on received-power measurements. In fact, proximity to absorber will affect all measurement in RCs. Thus, best-practice test guidelines should include specifications for DUT placement with respect to large-form-factor loads. Additionally, as discussed in the Introduction, when large-form-factor loads are present in the

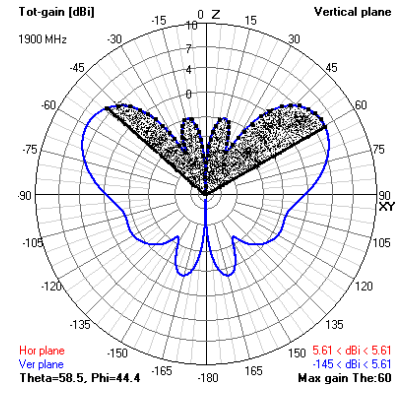


Figure 8. Finite element method-computed monopole antenna pattern, with typical blocked area shaded.

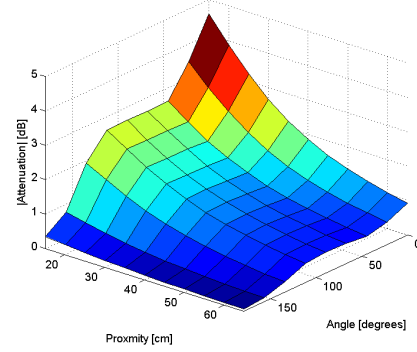


Figure 9. FEM-derived model for blockage pattern curve, for 14 absorber blocks

chamber, measurements should be made at multiple locations because of the potential for decreased spatial uniformity.

These results, particularly those presented in Fig. 5, present a starting point for a guideline for the placement of antennas on devices made up partially of lossy materials. However, they lack generality. Future work will consider how these results can be extrapolated into general guidelines.

The material presented in Section IV shows that a simple model could help physically explain the reduction in received power. This model, with refinements, can form a basis to inform design decisions for large-form-factor M2M devices incorporating lossy materials in the future. Possible refinements to the model include redesigning the model to also take into account primary and secondary reflections of radiation off the walls and ceiling of the chamber, which were not accounted for in the model used, or further refinement of the antenna pattern model itself, with a higher-grade modeling package or anechoic chamber measurements. From this new model, plots similar to Fig. 9 can be derived and used to develop placement guidelines.

Future research will study the influence of the proximity effect on the Q-factor measurement in a reverberation chamber. As shown in [4] and [19], different loading characteristics can have significant impact on the measured Q-factor of the chamber, suggesting that the proximity effect demonstrated in this paper may be present as well. Initial results are presented in [20].

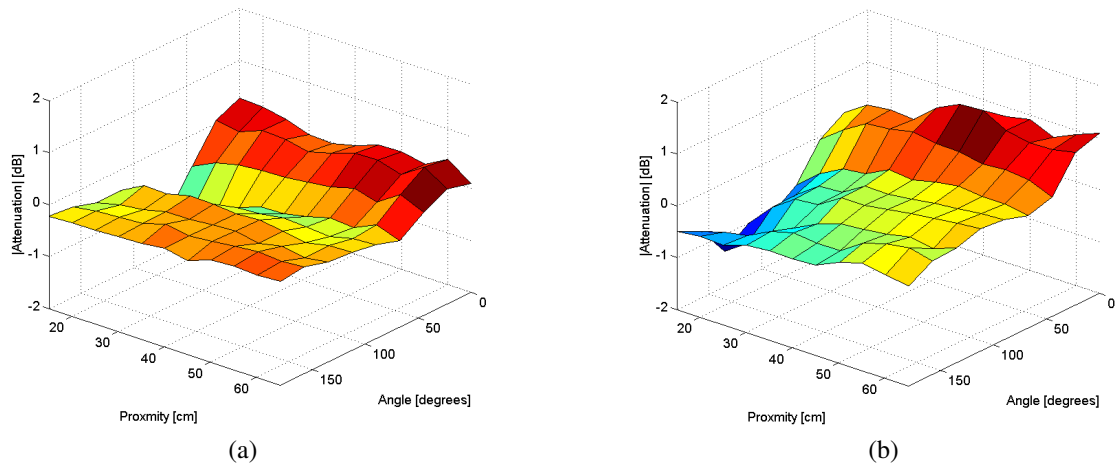


Figure 10. Difference between FEM-derived model and measurements: (a) four blocks, and (b) 14 blocks.

Table I
UNCERTAINTIES FOR REPRODUCIBILITY AND SPATIAL UNIFORMITY [9]

Load	$U_{L,measurement}$	$U_{L,loading}$	$U_{L,total}$
4	± 0.3 dB	± 0.19 dB	± 0.36 dB
8	± 0.3 dB	± 0.38 dB	± 0.48 dB
12	± 0.3 dB	± 0.56 dB	± 0.63 dB
14	± 0.3 dB	± 0.64 dB	± 0.71 dB

Table II
FREQUENCY AVERAGES OF RECEIVED POWER.

Location	Average received power [dB]
N	-27.57
S	-27.51
E	-27.69
W	-27.51

VI. ACKNOWLEDGEMENTS

The authors thank ETS-Lindgren for supplying the absorber blocks used in this work.

REFERENCES

- [1] C.L. Holloway, D.A. Hill, J.M. Ladbury, P.F. Wilson, G. Koepke, and J. Coder, "On the use of reverberation chambers to simulate a rician radio environment for the testing of wireless devices," *IEEE Trans. Electromagn. Compat.*, vol. 54, no. 11, Nov. 2006.
- [2] K. Rosengren, P.-S. Kildal, C. Carlsson, J. Carlsson, "Characterization of antennas for mobile and wireless terminals in reverberation chambers: improved accuracy by platform stirring", *Microwave Op. Technol. Lett.*, Vol. 30, no 20, pp. 391-397, Sep. 2001
- [3] M. Lienard, P. Degauque, "Simulation of dual array multipath channels using mode-stirred reverberation chambers", *Electron. Letters.*, vol. 40, no. 10, pp. 578-579, May 2004
- [4] E. Genender, C.L. Holloway, K.A. Remley, J. M. Ladbury, G. Koepke, and H. Garbe, "Simulating the multipath channel with a reverberation chamber: application to bit error rate measurements," *IEEE Trans. Electromagn. Compat.*, vol. 52, no. 4, pp. 766-777, Nov. 2010.
- [5] D.A. Hill, *Electromagnetic Fields in Cavities*. New York: IEEE Press, 2009.
- [6] D. Zhang, E. Li, "Loading effect of EUT on maximal electric field level in a reverberation chamber for immunity test," *IEEE 2002 International Symposium on EMC*, vol. 2, pp. 972-975, 19-23 Aug. 2002.
- [7] C.L. Holloway, D.A. Hill, J.M. Ladbury, and G. Koepke, "Requirements for an effective reverberation chamber: unloaded or loaded," *IEEE Trans. Electromagn. Compat.* vol. 48, no. 1, pp. 187-194, Feb. 2006.
- [8] J.M. Ladbury, P.F. Wilson, G.H. Koepke, and T. Lammers, "Reverberation chamber: An evaluation for possible use as a RF exposure system for animal studies," *Proc. Bio-Electromagnetics Society 25th Annual Meeting*, Maui, HI, Jun. 22-27, 2003.
- [9] S. Van de Beek, K.A. Remley, C.L. Holloway, J.M. Ladbury and F. Leferink, "Characterizing large-form-factor devices in a reverberation chamber", submitted to *EMC Europe*, 2013.
- [10] Electromagnetic compatibility (EMC) Part 4-21: Testing and Measurement Techniques Reverberation Chambers. *IEC Standard 61000-4-21*, 2003.
- [11] P. Corona, G. Ferrara, and M. Migliaccio, "Reverberating chamber electromagnetic field in presence of an unstirred component," *IEEE Trans. Electromagn. Compat.*, vol. 42, no. 2, pp. 111-115, May 2000.
- [12] C.L. Holloway, H.A. Haider, R.J. Pirkel, W. Young, D.A. Hill, and J. Ladbury, "Reverberation chamber techniques for determining the radiation and total efficiency of antennas," *IEEE Trans. Antennas and Propagation*, vol. 60, no. 4, pp. 1758-1770, April 2012
- [13] J.M. Ladbury, G. Koepke, and D. Camell, "Evaluation of the NASA Langley research center mode-stirred chamber facility," Nat. Inst. of Standards, Boulder, CO, 1999, *NIST Tech. Note 1508*.
- [14] J.M. Ladbury, D.A. Hill, "An improved model for antennas in reverberation chambers," *2010 IEEE Internat. Symp. on Electromagnetic Compatibility*, 25-30 July 2010, pp 663-667.
- [15] P.-S. Kildal, C. Carlsson, and J. Yang, "Measurement of free-space impedances of small antennas in reverberation chambers," *Microw. Opt. Technol. Lett.*, vol. 32, pp. 112-115, 2002.
- [16] J.M. Ladbury, D.A. Hill, "Enhanced backscatter in a reverberation chamber: inside every complex problem is a simple solution struggling to get out," *International Symposium on Electromagnetic Compatibility*, pp 1-5, 9-13 July 2007.
- [17] C.A. Balanis *Advanced Engineering Electromagnetics*, New York, N.Y.:Wiley, 1989.
- [18] C.L. Holloway, R.L. DeLyser, R.F. German, P. McKenna, M. Kanda, "Comparison of electromagnetic absorber used in anechoic and semi-anechoic chambers for emissions and immunity testing of digital devices", *IEEE Trans. Electromagn. Compat.* vol. 39, no. 1, pp 33-47 February 1997.
- [19] O. Lunden, M. Backstrom, "Absorber loading study in FOI 36.7 m3 mode stirred reverberation chamber for pulsed power measurements", *Proc. IEEE Int. Symp. Electromagn. Compat.*, Detroit, MI, Aug. 18-22, 2008, pp.1-5.
- [20] W.T.C. Burger, C.L. Holloway, K. A. Remley, "Influence on Q-factor of proximity and orientation with respect to farge-form-factor loads in a reverberation chamber", submitted to *EMC Europe*, 2013.